PROC. 15TH INT. CONF. PHYSICS OF SEMICONDUCTORS, KYOTO, 1980
J. PHYS. SOC. JAPAN **49** (1980) SUPPL. A p. 197–200

EFFECT OF MAGNETIC FIELD ON THE VALLEY-ORBIT SPLIT 1s STATES OF SHALLOW DONORS IN GERMANIUM

R.L. Aggarwal,† R. People, P.A. Wolff and David M. Larsen†

Massachusetts Institute of Technology
Cambridge, Massachusetts 02139
U.S.A.

We have studied the magnetic field dependence of the valley-orbit splitting, $4\Delta(B)$, between the $1s(A_1)$ and $1s(T_2)$ levels of P and As donors in Ge at 1.8°K with $n_D \sim 10^{15}$ cm^{-3}, using four-wave mixing spectroscopy. We find $4\Delta(B) = 4\Delta(0) + \alpha B^2$ for $B \lesssim 7T$, with $\alpha = 0.018$ cm^{-1}/T^2 for P and 0.027 cm^{-1}/T^2 for As. These values of α are consistent with theoretical estimates of the difference in the diamagnetic shifts for the $1s(T_2)$ and $1s(A_1)$ levels of isolated donors and reflect the breakdown of the effective mass approximation for the $1s(A_1)$ level.

I. Introduction

Valley-orbit splitting of the 1s ground state of group V donors (P, As, Sb, Bi) in germanium has been studied by a number of investigators. By observing transitions allowed in infrared absorption from the 1s levels to a common p level, Reuszer and Fisher [1] made an accurate determination of the valley-orbit splitting, 4Δ, between the nondegenerate ground state, $1s(A_1)$, and the upper 3-fold degenerate state, $1s(T_2)$. Forbidden optical absorption between the 1s states has been observed in the far infrared at photon energies corresponding to 4Δ for P and As donors [2,3]. Allowed spontaneous Raman scattering between the 1s states has also been studied [4]. Four-wave mixing spectroscopy (FWMS), one of the techniques of coherent Raman scattering which offers several advantages over spontaneous Raman scattering [5], has been applied previously for the high-resolution study of the $1s(A_1) \rightarrow 1s(T_2)$ transition in zero magnetic field [6]. In FWMS experiments, two laser beams at frequencies ω_1 and ω_2 interact simultaneously with donors to generate radiation at frequency $\omega_4 = 2\omega_1 - \omega_2$ via the third-order susceptibility, χ^3. When $\hbar(\omega_1 - \omega_2)$ becomes equal to 4Δ, $\chi^{(3)}$ and, hence, the intensity of the ω_4 radiation exhibits a peak.

In this paper we report measurements of the energy separation, $4\Delta(B)$, between the $1s(A_1)$ and $1s(T_2)$ levels as a function of the magnetic field, $\vec{B}$, applied along a [100] crystal axis for P and As donors in Ge, using FWMS. $\vec{B}$ was chosen along [100] since in that orientation it does not lift the degeneracy of the $1s(T_2)$ levels (ignoring spin effects) and, therefore, provides the simplest possible spectrum. Experimental procedure and results are presented in Sec. II. Theory and discussion of results is given in Sec. III.

---

†Francis Bitter National Magnet Laboratory supported by the National Science Foundation.

II. Experimental

A schematic of the experimental setup for FWMS is shown in Fig. 1. 200 ns CO_2 laser pulses of about 1 kW maximum peak power at frequencies ω_1 and ω_2 are provided simultaneously by using a pair of intercavity mirrors mounted on the opposite sides of a shaft rotating at 150 Hz. Following the Ge beamsplitter, the two laser beams propagate collinearly and are focused on a ~0.6 cm long Ge sample at 1.8°K with a BaF_2 lens into ~200 μm spot. Each laser beam incident on the sample has typical peak power of ~200W, with electric vector $\vec{E}_1 \parallel \vec{E}_2 \perp \vec{B}$ and propagation vector $\vec{k} \perp \vec{B}$. The ω_4-signal is resolved from the two incident laser beams with a Spex double grating monochromator and is measured with a Cu-doped Ge photodetector. The output of the detector is averaged by a boxcar integrator and displayed on a strip-chart recorder.

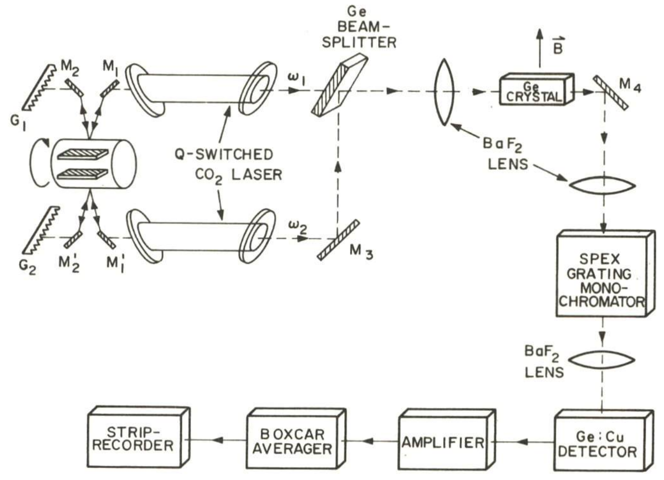

Fig. 1 Schematic of the experimental setup for FWMS in a magnetic field

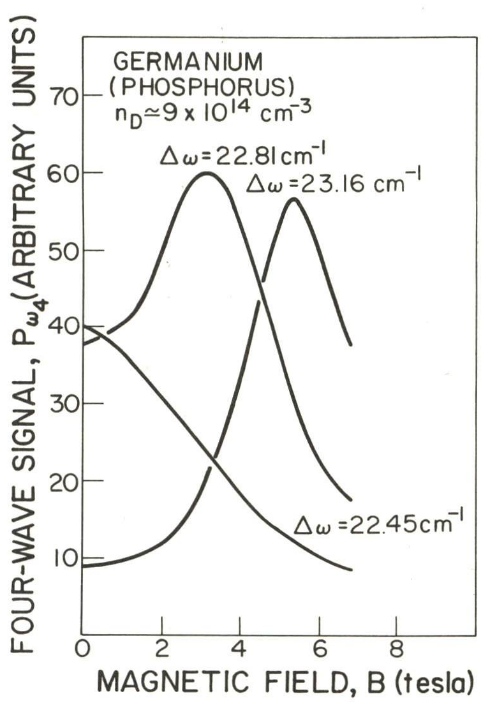

Fig. 2 Four-wave signal, $P\omega_4$, vs. applied magnetic field $\vec{B} \parallel [100]$ in Ge at 1.8°K

For a fixed laser frequency difference $\Delta\omega = \omega_1 - \omega_2$, the ω_4-signal, $P\omega_4$, is measured as a function of B. For $\Delta\omega > 4\Delta(0)$, $P\omega_4$ shows a maximum at a value of B which satisfies the resonance condition $\hbar\Delta\omega = 4\Delta(B)$. Figure (2) shows the tuning curves obtained for three different values of $\Delta\omega$ for P-doped Ge. Note that no peak is observed for $\Delta\omega = 22.45$ cm^{-1}, which is less than $4\Delta(0)$ for P donors. A plot of $4\Delta(B)$ vs. B^2 is shown in Fig. (3) (on the last page) for P and As donors. The solid lines in Fig. (3) represent a least-squares straight line fit to the data, giving $4\Delta(B) = 4\Delta(0) + \alpha B^2$ with $4\Delta(0) = 22.6$ cm^{-1} for P and 34.0 cm^{-1} for As. Values of the coefficient α are given in Table I in the following section.

III. Theory and Discussion of Results

In the effective mass approximation (EMA) $4\Delta(B) = 0$ and the $1s(A_1)$ and $1s(T_2)$ states have identical envelope functions. We present arguments indicating that the observed magnetic field dependence of $4\Delta(B)$ discussed in Sec. II is the result of smallness of the spread of the true $1s(A_1)$ envelope functions relative to those of the $1s(T_2)$ levels, which are nearly effective mass like.

A useful donor variational trial envelope function in the EMA for a given valley, i, can be written

$$\chi_i = A\exp\left(-\delta^2 z_i^2 - \kappa\left(\rho_i^2 + \alpha z_i^2\right)^{\frac{1}{2}}\right) , \tag{1}$$

where z_i lies along the axis of cylindrical symmetry of the energy ellipsoid of valley i, and A is a normalization factor. The "best" choice of variational parameters in eq. (1) leads to an EMA energy, $\tilde{R}$, of -2.0884 R, where $R = m_\perp e^4/2\varepsilon_0^2\hbar$; here we have used $\sigma \equiv m_\perp/m_z = 0.05134$ [7] where $m_\perp$ and m_z are effective masses for motion in valley i perpendicular and parallel, respectively, to z_i. If $\vec{B}$ lies along [100], it makes an angle of $\cos^{-1}(1/\sqrt{3})$ with z_i for all four valleys. In that case the diamagnetic shift is not proportional to $<\rho_i^2>$ as it would be for the ground state of a donor in a spherical band but is given approximately by [8]

$$\delta E = R\left[\left(\gamma_z^2/4 + \sigma(1-\xi)^2\gamma_\perp^2/2\right)<\rho_i^2> + \xi^2\gamma_\perp^2<z_i^2>\right] , \tag{2}$$

where $\xi = \sigma <\rho_i^2>/(\sigma<\rho_i^2> + 2<z_i^2>)$, <> denotes expectation value in χ_i, all lengths are in units of the Bohr radius $\hbar^2\varepsilon_0/m_\perp e^2$, and γ_z and $\gamma_\perp$ are dimensionless components of B, along and perpendicular, respectively, to z_i and defined by $\gamma_{z,\perp} = (\hbar eB_{z,\perp}/m_\perp c)/(2R)$. Equation (2) is valid in the EMA for arbitrary direction of $\vec{B}$. Specializing to the case that $\vec{B}$ lies along [100] we find that eq.(2) gives the same diamagnetic shift for all four valleys, which becomes $0.0727\gamma^2 R$; this corresponds to an energy shift of $0.0633\ cm^{-1}/T^2$. Equation (2) is derived by introducing the gauge

$$\vec{A} = B_z\left(-y_i/2, x_i/2, 0\right) + B_\perp\left(\xi z_i, 0, -(1-\xi)x_i\right) , \tag{3}$$

into the effective mass Schrödinger equation for the donor electron in valley i. In eq. (3) the y_i axis has been implicity chosen along $\vec{B}_\perp$; the value of ξ to be inserted in eq.(2) is obtained by minimizing δE with respect to ξ.

The true envelope function for valley i in the actual A_1 ground state is not χ_i but a function which is much more strongly concentrated at the donor center than is χ_i. Given the observed zero-field energy of the A_1 state, it should be possible in principle to calculate this state at points outside the range of the short-range central cell force responsible for the breakdown of the EMA. For <u>spherical</u> valleys this function is known to be given by $\phi = W_{n,\frac{1}{2}}(2r/n)/r$, where $n = (1/E)^{\frac{1}{2}}$, E is the observed energy of the ground state in units of $\tilde{R}$ (E = 1.31 for P and 1.44 for As in Ge [1,7]) and $W_{n,\frac{1}{2}}$ is a Whittaker function [9]. For nonspherical valleys like those of Ge the appropriate envelope functions are unknown.

To estimate the diamagnetic shift associated with the wave function in the i-th valley we employ eq.(2) but reduce the quantities $<\rho_i^2>$ and $<z_i^2>$ appearing there by multiplying them with the scale factor $<\phi|r^2|\phi>/(3<\phi|\phi>)$, where we have used $\int d^3r\, r^2 e^{-2r}/\int d^3r e^{-2r} = 3$. This follows from assuming that the shrinkage of the mean value of

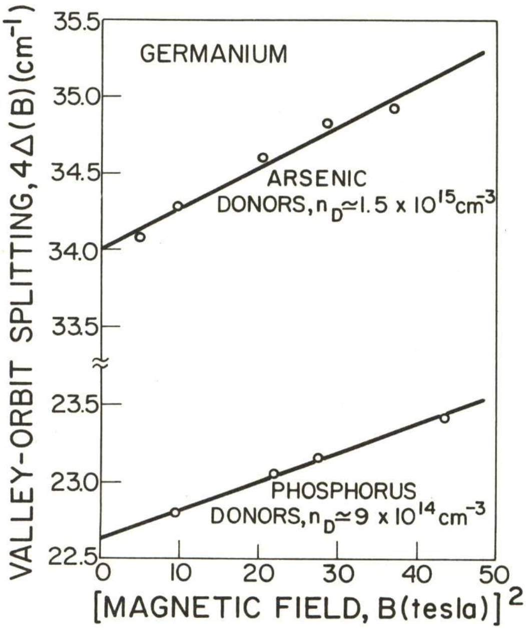

Fig. 3 Valley-splitting in a [100] magnetic field vs. B^2

r^2 in the true envelope function for given E, relative to the EMA wave function is independent of the mass anisotropy of the valley and that the ratio of mean z_i^2 in the true envelope function is $\langle z_i^2 \rangle / \langle \rho_i^2 \rangle$ (i.e. the same as that in the EMA). For the $1s(A_1)$ and $1s(T_2)$ states of Ge:P we obtain scale factors of 0.582 and 0.947, respectively; the corresponding factors for Ge:As are 0.488 and 0.969. From these numbers and the EMA shift of 0.0633 cm^{-1}/T^2 from eq.(2) we obtain the theoretical values in Table I.

The agreement of experiment and theory indicated in Table I supports our contention that the magnetic field dependence of the A_1-T_2 splitting for isolated donors is due primarily to the different orbital diamagnetism of these states.

Table I Comparison of predicted and observed values of $\alpha(cm^{-1}/T^2)$

Donor	$n_D(cm^{-3})$	α Theory	α Experiment
P	9×10^{14}	0.023	0.018±.002
P	1×10^{16}	---	0.029±.002
As	1.5×10^{15}	0.030	0.027±.002

The higher value of α for the 1×10^{16} cm^{-3} P-sample is presumably connected with delocalization. However, a real understanding of this effect is lacking at the present time.

References

1. J.H. Reuszer and P. Fisher: Phys. Rev. 135 (1964) A1125.
2. V.V. Buzdin, A.I. Demeshina, Y.A. Kurskii and V.N. Murzin: Sov. Phys.-Semiconductors 6 (1973) 1792.
3. M. Kobayashi and S. Narita: J. Phys. Soc. Japan 43 (1977) 1455.
4. J. Doehler, P.J. Colwell and S.A. Solin: Phys. Rev. Lett. 34 (1975) 584.
5. M.D. Levenson: Physics Today May (1977) 44.
6. R.A. Wood, M.A. Khan, P.A. Wolff and R.L. Aggarwal: Opt. Commun. 21 (1977) 154.
7. R.A. Faulkner: Phys. Rev. 184 (1969) 713. See especially Table VIII.
8. D.M. Larsen: unpublished calculations.
9. W. Kohn and J.M. Luttinger: Phys. Rev. 97 (1955) 883.